

Studies of Radiative Penguin Decays at *BABAR*.

Colin P. Jessop (for the *BABAR* collaboration.)^a

^aStanford Linear Accelerator Center, 2575 Sand Hill Road,
 Menlo Park, CA 94025, U.S.A.

The electromagnetic radiative “penguin” decays $b \rightarrow s\gamma$, $b \rightarrow d\gamma$ are sensitive to physics beyond the Standard Model. We present recent studies made with the *BABAR* detector at the PEP-II asymmetric e^+e^- storage ring.

1. Introduction

The radiative $b \rightarrow s\gamma$, $b \rightarrow d\gamma$ transitions occur by the electromagnetic “penguin” loop diagram in the Standard Model. These decays are sensitive to the CKM matrix elements V_{td} and V_{ts} and to new virtual high mass particles such as a charged Higgs appearing in the loop causing deviations in the rate [1] and possibly introducing a new CP -violating phase. The Standard Model predictions [2] for the leading exclusive decays $B \rightarrow K^*\gamma$ ($b \rightarrow s\gamma$) and the as yet unobserved $B \rightarrow \rho\gamma$ ($b \rightarrow d\gamma$) decay suffer from large uncertainties compromising the sensitivity to both CKM matrix elements and new physics. However in the ratio $\mathcal{B}(B \rightarrow \rho\gamma)/\mathcal{B}(B \rightarrow K^*\gamma)$ some of these uncertainties cancel and a competitive measurement of V_{ts}/V_{td} is possible. We present measurements of the exclusive decay, $\mathcal{B}(B \rightarrow K^*\gamma)$ [5], the CP -violating charge asymmetry, $A_{cp}(B \rightarrow K^*\gamma)$ and results of a search for $B \rightarrow \rho\gamma$ and $B \rightarrow \omega\gamma$ [6].

The predictions for the inclusive rates [3] are more precise as quark-hadron duality is believed to be a good approximation so that $B \rightarrow X_s\gamma = b \rightarrow s\gamma$. We present two measurements of $\mathcal{B}(B \rightarrow X_s\gamma)$ using both a semi-inclusive [8] and a fully inclusive technique [7]. The photon energy spectrum from the $B \rightarrow X_s\gamma$ measured with the semi-inclusive technique is also used to extract values for the HQET parameters $\bar{\lambda}$ and λ_1 .

The data were collected with the *BABAR* detector [9] at the PEP-II asymmetric $e^+(3.1 \text{ GeV}) - e^-(9 \text{ GeV})$ storage ring. We use Monte Carlo simulations of the *BABAR* detector based on GEANT 4.0 [10] to optimize our selection criteria, to deter-

mine signal efficiencies, and in some cases to estimate backgrounds. These simulations take account of varying detector conditions and beam backgrounds.

The event selection for both the exclusive and inclusive analysis begins by requiring a high-energy radiative photon candidate. A photon candidate is defined as a localized energy maximum in the calorimeter. It must be isolated by from any other photon candidate or track and have a lateral energy profile consistent with a photon shower. We veto photons from a $\pi^0(\eta)$.

2. $\mathcal{B}(B \rightarrow K^*\gamma)$ and $A_{cp}(B \rightarrow K^*\gamma)$

The details of the event selection are described in [5]. The K^* is reconstructed from K^+ , K_s^0 , π^- and π^0 candidates through the four modes $K^{*0} \rightarrow K^+\pi^-$, $K_s^0\pi^0$ and $K^{*+} \rightarrow K^+\pi^0$, $K_s^0\pi^+$ and combined with a high energy photon to form a B meson candidate. The dominant background is from continuum production from continuum $q\bar{q}$ production, where q can be a u, d, s or c quark, with the high-energy photon originating from initial-state radiation or from π^0 and η decays. The continuum background is produced above threshold and so is lorentz boosted to a “jet-like” topology in contrast to the signal which is produced isotropically. Event topology variables are used to suppress the background. Finally we construct from the B candidates two independent variables ΔE and m_{ES} used to extract the signal yield. We define $\Delta E = E_B^* - E_{beam}$ and $m_{ES} = \sqrt{E_{beam}^{*2} - p_B^{*2}}$ where E_B^* and p_B^* are the energy and momentum of the reconstructed

B , computed in the center of mass frame of the e^+e^- and E_{beam} is the precisely known beam energy. These variables exploit the fact that the beam energy is equal to the energy of the produced B but more accurately known than the detector reconstructed energy measurement.

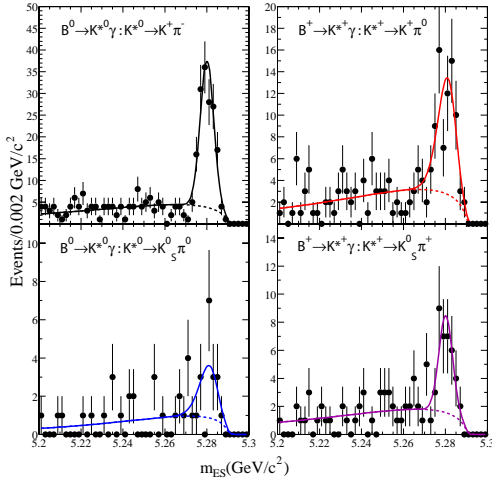


Figure 1. m_{ES} for the $B \rightarrow K^*\gamma$ candidates. The solid and dashed curves show respectively the fitted signal-plus-background and the background alone.

The analysis is performed on 22.7 million $B\bar{B}$ pairs. Figure 1 shows the m_{ES} distributions for the four decay modes. The signal is extracted from a maximum likelihood fit. The background is modeled by a threshold function [4]. The measured branching fractions and CP – violating charge asymmetries are summarised in Table 1. The branching fractions are roughly a factor of two lower than the next-to-leading order Standard Model predictions and in agreement with previous measurements [11].

3. Search for $B \rightarrow \rho\gamma$ and $B \rightarrow \omega\gamma$

The analysis, described in detail in reference [6], is considerably more challenging than the $B \rightarrow K^*\gamma$ measurements. The signal rate is

Table 1

The measured branching fraction $\mathcal{B}(B \rightarrow K^*\gamma)$ and A_{CP} for each of the decay modes.

Mode	$\mathcal{B}(B \rightarrow K^*\gamma)$ - \pm stat. \pm sys. $\times 10^{-5}$	$A_{CP}(\text{signal})$ (\pm stat. \pm sys.)
$K^+\pi^-$	$4.24 \pm 0.41 \pm 0.22$	$-0.049 \pm 0.094 \pm 0.012$
$K_S^0\pi^0$	$4.10 \pm 1.71 \pm 0.42$	
$K_S^0\pi^+$	$3.01 \pm 0.76 \pm 0.21$	$-0.190 \pm 0.210 \pm 0.012$
$K^+\pi^0$	$5.52 \pm 1.07 \pm 0.38$	$0.044 \pm 0.155 \pm 0.021$

expected to be of order 50 times smaller than $B \rightarrow K^*\gamma$ ($\mathcal{B}[B^+ \rightarrow \rho^+\gamma] = (0.9 - 1.5) \times 10^{-6}$ [2]) with significantly higher continuum backgrounds and additional backgrounds from $b \rightarrow s\gamma$ processes. The decay $B \rightarrow \rho\gamma$ is reconstructed with $\rho^0 \rightarrow \pi^+\pi^-$ and $\rho^+ \rightarrow \pi^+\pi^0$, while $B^0 \rightarrow \omega\gamma$ is reconstructed with $\omega \rightarrow \pi^+\pi^-\pi^0$. Continuum backgrounds are suppressed with event topology variables, vertexing and flavor tagging. The variables are combined into a neural net, trained on Monte Carlo, and validated with several data control samples. A dedicated pion selector has been developed for this analysis optimized to reject the kaon fake background from $b \rightarrow s\gamma$ processes. The analysis was performed “blind” on 84.4 million BB pairs. Figure 2 shows the $\Delta E, m_{ES}$ dsitributions for the data after all cuts. The signal yield is estimated from a multi-dimensional maximum likelihood fit. The results are given in table 2. No signal is observed and we set 90 % confidence limits.

Table 2

The signal yields and errors obtained from the signal extraction fit, and the 90 % Confidence Limit.

Mode	Yield (Events)	90% C.L. $\times 10^{-6}$
$B^0 \rightarrow \rho^0\gamma$	4.8 ± 5.2	1.4
$B^+ \rightarrow \rho^+\gamma$	6.2 ± 5.5	2.3
$B^0 \rightarrow \omega\gamma$	0.1 ± 2.3	1.9

The limits for the individual modes can be combined assuming isospin symmetry to give $\mathcal{B}(B \rightarrow \rho\gamma) < 1.9 \times 10^{-6}$ at 90 % C.L.. In addition this limit can be compared to the measured $\mathcal{B}(B \rightarrow$

$K^*\gamma$) above to give $\mathcal{B}(B \rightarrow \rho\gamma)/\mathcal{B}(B \rightarrow K^*\gamma) < 0.047$ at 90 % C.L.

4. Measurement of $\mathcal{B}(B \rightarrow X_s\gamma)$ using a “semi-inclusive” technique

The fragmentation of the s-quark in the $b \rightarrow s\gamma$ transition results in final states, X_s , containing kaons and pions proceeding through a complicated resonance structure. One technique to measure the inclusive rate is to attempt to reconstruct all possible X_s states. However, we are not sensitive to states containing a K_L^0 while the prohibitively large combinatorics from high multiplicity modes and modes with $K_S^0 \rightarrow \pi^0\pi^0$ limit the fraction of accessible modes to approximately 50 %. We reconstruct the X_s in the $K^+\pi^-$, $K_S^0\pi^0$, $K^+\pi^-\pi^0$, $K_S^0\pi^+\pi^-$, $K^+\pi^-\pi^+\pi^-$, $K_S^0\pi^+\pi^-\pi^0$, $K^+\pi^0$, $K_S^0\pi^+$, $K^+\pi^-\pi^+$, $K_S^0\pi^+\pi^0$, $K^+\pi^-\pi^+\pi^0$, $K_S^0\pi^+\pi^-\pi^+$ modes in 22.7 million $B\bar{B}$ pairs. The basic reconstruction technique is

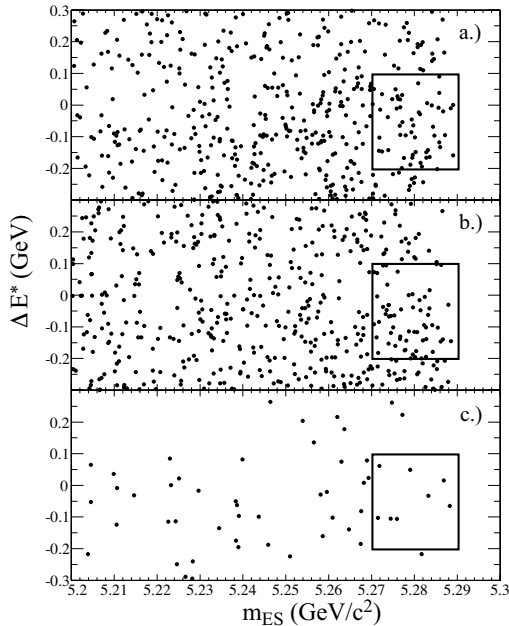


Figure 2. ΔE vs. m_{ES} for a.) $B^0 \rightarrow \rho^0\gamma$, b.) $B^+ \rightarrow \rho^+\gamma$ and c.) $B^0 \rightarrow \omega\gamma$ candidates. The boxes indicate the blinded region.

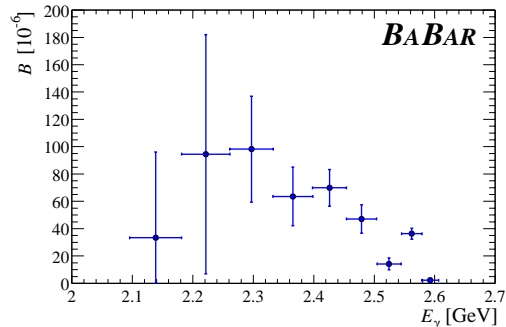


Figure 3. Branching fraction as a function of E_γ . The errors are purely statistical.

essentially the same as for the $B \rightarrow K^*\gamma$ analysis described above, except that there are additional backgrounds from $B\bar{B}$ decays and cross-feed between the modes. The analysis is described in detail in reference [8]. The X_s is divided into several m_{X_s} (dual to E_γ^*) bins and the signal yield extracted from a fit to m_{ES} for each of these bins. Figures 3 and 4 show the resultant E_γ^* and

m_{X_s} spectra respectively. The first moment of the E_γ^* spectra can be used to extract a measurement of the HQET parameter $\bar{\Lambda}(\alpha_s^2, 1/M_B^3)$ [13]. We find $\langle E_\gamma \rangle |_{E_\gamma > 2.094 \text{ GeV}} = 2.35 \pm 0.04 \text{ (stat)} \pm 0.04 \text{ (syst)} \text{ GeV}$ from which we derive $\bar{\Lambda} = 0.37 \pm 0.09 \text{ (stat)} \pm 0.07 \text{ (syst)} \pm 0.10 \text{ (model)} \text{ GeV}$. The parameter $\bar{\Lambda}$ then provides information to help constrain the parameters in the fit to the m_{X_s} spectrum shown in fig 4 used to extract $\mathcal{B}(b \rightarrow s\gamma) = 4.3 \pm 0.5 \text{ (stat)} \pm 0.8 \text{ (syst)} \pm 1.3 \text{ (model)} \cdot 10^{-4}$ and $\lambda_1 = -0.24^{+0.03}_{-0.04} \text{ (stat)} \pm 0.02 \text{ (syst)}^{+0.15}_{-0.21} \text{ (model)} [\text{GeV}/c^2]^2$, consistent with standard model predictions [3] and previous measurements [12]. Note that this technique gives large systematic errors due to uncertainties in the fragmentation model and resonance structure of the X_s .

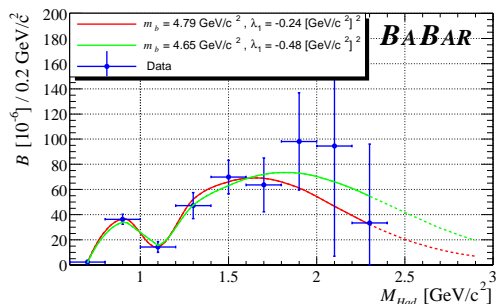


Figure 4. Superposition of the predicted spectrum for $m_b = 4.79 \text{ GeV}/c^2$ and $m_b = 4.65 \text{ GeV}/c^2$ on the observed hadronic mass spectrum.

5. Measurement of $\mathcal{B}(B \rightarrow X_s\gamma)$ using a “Fully-inclusive” technique

The semi-inclusive measurement of $\mathcal{B}(B \rightarrow X_s\gamma)$ offers a powerful technique to suppress backgrounds but the sensitivity to the details of the X_s fragmentation incurs large systematic uncertainties. A fully inclusive measurement sensitive to 100 % of the decay is highly desirable but complicated by the large backgrounds as shown

in Figure 5. Here for pedagogical purposes we have selected a high energy photon using standard quality cuts from a sample of signal and continuum and $B\bar{B}$ Monte Carlo. To reduce

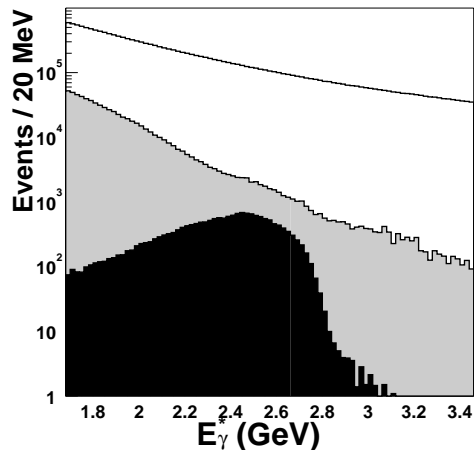


Figure 5. The energy distribution, in the $\Upsilon(4s)$ center of mass, of simulated photon candidates, after “photon quality” cuts. Shown are $B \rightarrow X_s\gamma$ signal (dark shading), $B\bar{B}$ background (grey shading) and continuum background (unshaded), all normalized to 54.6 Million BB.

these backgrounds while remaining insensitive to the X_s fragmentation we employ a lepton tagging technique. The analysis is described in detail in reference [7]. The tagging reduces the continuum background by 3 orders of magnitude but at a cost of low efficiency ($\approx 0.5\%$). Also a significant $B\bar{B}$ background remains which must be estimated by Monte Carlo. Figure 6 shows the E_γ^* spectrum for data with the estimated background. We find $\mathcal{B}(B \rightarrow X_s\gamma) = 3.88 \pm 0.36 \text{ (stat.)} \pm 0.37 \text{ (syst.)} \pm 0.23^{0.43}_{-0.23} \text{ (model)} \times 10^{-4}$. The dominant systematic uncertainty is from the modelling of the $B\bar{B}$ background which has been compared to data control samples. The measurement is consistent with both Standard Model expectations [3] and previous measurements [12]

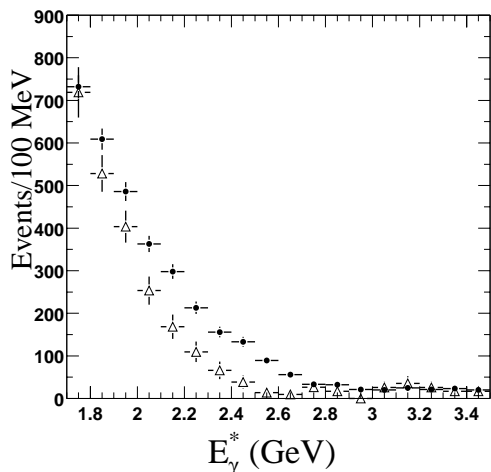


Figure 6. The E_γ^* distribution of on-resonance data (solid points) compared to background expectation. All errors are statistical only.

REFERENCES

1. See for example, S. Bertolini, F. Borzumati and A. Masiero, Nucl. Phys. B **294**, 321 (1987); H. Baer, M. Brhlik, Phys. Rev. D **55**, 3201 (1997); J. Hewett and J. Wells, Phys. Rev. D **55**, 5549 (1997); M. Carena *et al.*, Phys. Lett. B **499**, 141 (2001).
2. Z. Ligeti and M. B. Wise, Phys. Rev. D **60**, 117506 (1999); M. Beneke, T. Feldmann and D. Seidel; Nucl. Phys. B **612**, 25 (2001) S. W. Bosch and G. Buchalla, Nucl. Phys. B **621**, 459 (2002); A. Kagan and M. Neubert, e-print hep-ph/0110078(2001); A. Ali and A. Y. Parkhomenko, Eur. Phys. J. C **23**, 89 (2002). B. Grinstein and D. Pirjol, Phys. Rev. D **62**, 093002 (2000).
3. K. Abel and Y. P. Yao, Phys. Rev. D **49**, 4945 (1994); A. Ali and C. Greub, Phys. Lett. B **361**, 146 (1995); C. Greub and T. Hurth, Phys. Lett. B **380**, 2934 (1997); C. Greub, T. Hurth and D. Wyler, Phys. Lett. B **361**, 385 (1996); K. Chetyrkin, M. Misiak and M. Munz, Phys. Lett. B **400**, 296 (1997); A. J. Buras, A. Kwiatkowski and N. Pott, Phys. Lett. B **414**, 157 (1997); A. Kagan and M. Neubert, Eur. Phys. Journal **7** 5 1999 ; A. Kagan and M. Neubert, Phys. Rev. D **58**, 094012 (1998); P. Gambino and M. Misiak, Nucl. Phys. B **611**, 338 (2001).
4. ARGUS Collaboration, H. Albrecht *et al.*, Z. Phys. C **48**, 543 (1990).
5. “Measurement of $B \rightarrow K^*\gamma$ Branching Fractions and Charged Asymmetries” The BaBar Collaboration, B. Aubert *et al.* Phys. Rev. Lett. **88**, 101805 (2002).
6. “Search for the Exclusive Radiative Decays $B \rightarrow \rho\gamma$ and $B^0 \rightarrow \omega\gamma$.” The BaBar Collaboration, B. Aubert *et al.* e-print hep-ex/0207073.
7. “Determination of the Branching Fraction for Inclusive Decays $B \rightarrow X_s\gamma$.” The BaBar Collaboration, B. Aubert *et al.* e-print hep-ex/0207076.
8. “ $B \rightarrow X_s\gamma$ Using a Sum of Exclusive Modes.” The BaBar Collaboration, B. Aubert *et al.* e-print hep-ex/0207074.
9. “The BaBar Detector” The BaBar Collaboration, B. Aubert *et al.* Nucl. Instrum. Methods **A**, 479 (1)2002 .
10. “GEANT Detector Description and Simulation Tool”, CERN Program Library Long Writeup W5013 (1994).
11. T.E. Coan *et al.* [CLEO Collaboration], Phys. Rev. Lett. **84**, 5283 (2000); Y. Ushiroda *et al.* [BELLE Collaboration], contributed to BCP4, Ago Town, Japan, Feb 2001. hep-ex/0104045.
12. CLEO Collaboration, M.S. Alam *et al.*, Phys. Rev. Lett. **74**, 2885 (1995); ALEPH Collaboration, R. Barate *et al.*, Phys. Lett. B **429**, 169 (1998); BELLE Collaboration, K. Abe *et al.*, Phys. Lett. B **511**, 151 (2001); CLEO Collaboration, S. Chen *et al.*, Phys. Rev. Lett. **87**, 251807 (2001).
13. Z. Ligeti, M.E. Luke, A.V. Manohar, M.B. Wise, Phys. Rev. D **60**, 034019 (1999); C. Bauer, Phys. Rev. D **57**, 5611 (1998).